Published in final edited form as:
Neuroscience. 2011 March 31; 178: 196–207. doi:10.1016/j.neuroscience.2011.01.039.

THE MAJORITY OF MYELINATED AND UNMYELINATED SENSORY NERVE FIBERS THAT INNERVATE BONE EXPRESS THE TROPOMYOSIN RECEPTOR KINASE A

Gabriela Castañeda-Corral[1,2], **Juan M. Jimenez-Andrade**[1], **Aaron P. Bloom**[1], **Reid N. Taylor**[1], **William G. Mantyh**[1], **Magdalena J. Kaczmarska**[1], **Joseph R. Ghilardi**[3], and **Patrick W. Mantyh**[1,3,4]

[1] Department of Pharmacology, College of Medicine, University of Arizona, Tucson, AZ 85724, USA

[2] Departamento de Farmacobiología, Centro de Investigación y de Estudios Avanzados (Cinvestav), Sede Sur, México, DF, Mexico

[3] Research Service, VA Medical Center, Minneapolis, MN 55417, USA

[4] Arizona Cancer Center, University of Arizona, Tucson, AZ 85724, USA

Abstract

Although skeletal pain is a leading cause of chronic pain and disability, relatively little is known about the specific populations of nerve fibers that innervate the skeleton. Recent studies have reported that therapies blocking nerve growth factor (NGF) or its cognate receptor, tropomyosin receptor kinase A (TrkA) are efficacious in attenuating skeletal pain. A potential factor to consider when assessing the analgesic efficacy of targeting NGF-TrkA signaling in a pain state is the fraction of NGF-responsive $TrkA^+$ nociceptors that innervate the tissue from which the pain is arising, as this innervation and the analgesic efficacy of targeting NGF-TrkA signaling may vary considerably from tissue to tissue. To explore this in the skeleton, tissue slices and whole mount preparations of the normal, adult mouse femur were analyzed using immunohistochemistry and confocal microscopy. Analysis of these preparations revealed that 80% of the unmyelinated/thinly myelinated sensory nerve fibers that express calcitonin gene-related peptide (CGRP) and innervate the periosteum, mineralized bone and bone marrow also express TrkA. Similarly, the majority of myelinated sensory nerve fibers that express neurofilament 200 kDa (NF200) which innervate the periosteum, mineralized bone and bone marrow also co-express TrkA. In the normal femur, the relative density of $CGRP^+$, $NF200^+$ and $TrkA^+$ sensory nerve fibers per unit volume is: periosteum > bone marrow > mineralized bone > cartilage with the respective relative densities being 100: 2: 0.1: 0. The observation that the majority of sensory nerve fibers innervating the skeleton express $TrkA^+$, may in part explain why therapies that block NGF/TrkA pathway are highly efficacious in attenuating skeletal pain.

Corresponding author: Patrick W. Mantyh, Ph D, Department of Pharmacology, College of Medicine, University of Arizona, 1656 E. Mabel, Rm. #119, PO Box 245215, Tucson, AZ 85724, Phone: (520) 626-0742, Fax: (520) 626-8869, pmantyh@.arizona.edu.

Keywords

fracture pain; osteoarthritis; cancer pain; nerve sprouting

Skeletal pain is caused by a highly diverse group of disorders and conditions including fracture, osteoarthritis, vertebral degeneration, sickle cell anemia and chemotherapy (Giaccone et al., 1994, Morrison et al., 2003, Woolf and Pfleger, 2003, Aguilar et al., 2005, Kidd, 2006, Freemont, 2009). These skeletal pain states can significantly impair physical function and, if not effectively controlled, can lead to long-term disability (Lubeck, 2003, Morrison et al., 2003, Woolf and Pfleger, 2003, Rosemann et al., 2007). Importantly, in addition to the pain and physical disability brought about by skeletal injury/disease, skeletal pain can produce significant secondary effects including a reduction in mobility, cardiovascular function and cognitive health, all of which diminish the patient's functional status and quality of life (Woolf and Pfleger, 2003, Dominick et al., 2004, Sawatzky et al., 2007).

Given the high prevalence and impact of skeletal pain on society, it is surprising how little is known about the mechanisms that drive skeletal pain and how few therapies are available to treat this pain. Our lack of knowledge of what drives skeletal pain is in large part due to the difficulty of working with nerves in a calcified tissue such as bone (Mullink et al., 1985, Mach et al., 2002). It is well known that primary afferent and sympathetic neurons innervate the marrow, mineralized bone and the periosteum in both humans and rodents (Bjurholm et al., 1988, Wojtys et al., 1990, Hill and Elde, 1991, Hukkanen et al., 1992, Mach et al., 2002). Furthermore, it has been reported that the skeleton is innervated by peptide-rich C-fibers and thinly myelinated fibers, while largely lacking innervation by thickly mylelinated A-beta fibers and peptide-poor C-fibers (Seike, 1976, Kruger et al., 1989, Ozawa et al., 2003, Aoki et al., 2005, Zylka et al., 2005, Ivanusic et al., 2006, Mahns et al., 2006, Ozawa et al., 2006, Kuniyoshi et al., 2007, Ohtori et al., 2007, Nakajima et al., 2008, Jimenez-Andrade et al., 2010b). However, remarkably little is known about what neurotransmitters, receptors and ion channels these nerve fibers express, and whether the density, morphology, phenotype, and response characteristics change following injury and/or disease.

Recent preclinical data suggest that therapies blocking nerve growth factor (NGF) or its cognate receptor, tropomyosin receptor kinase A (TrkA) are more effective at attenuating skeletal pain versus skin pain. In animal models of arthritis (Shelton et al., 2005, McNamee et al., 2010), bone fracture (Jimenez-Andrade et al., 2007, Ghilardi et al., 2010b), and several models of bone cancer (Sevcik et al., 2005, Ghilardi et al., 2010a, Jimenez-Andrade et al., 2010a, Mantyh et al., 2010), blocking NGF or TrkA results in approximately 50% reduction in pain related behaviors. In contrast, in a skin incision model of pain, blocking NGF reduced thermal pain by 25% with no significant reduction in mechanical allodynia (Zahn et al., 2004). In agreement with these preclinical studies, human clinical trials where patients with moderate to severe osteoarthritis pain received an anti-NGF sequestering therapy, have shown approximately 50% reduction in walking pain (Lane et al., 2010). One explanation as to why blocking NGF or TrkA may be more effective in skeletal vs. skin pain is that compared to the skin the skeleton may be innervated by a select group of nociceptors, the majority of which express TrkA. To explore this possibility, the expression of TrkA in sensory nerve fibers that innervate the mouse femur was examined using immunohistochemistry and confocal microscopy. Additionally, the density/unit volume of $CGRP^+$, $NF200^+$ and $TrkA^+$ sensory nerve fibers was determined in the different compartments of the mouse femur.

EXPERIMENTAL PROCEDURES

Mice

Experiments were performed using 36 male C3H/HeJ mice weighing 20–25 g (Jackson Laboratories, Bar Harbor, ME, USA). The mice were housed in accordance with the NIH guidelines with a 12 h alternating light and dark cycle and were given food and water *ad libitum*. All procedures were approved by the Institutional Animal Care and Use Committee at the University of Arizona (Tucson, AZ) and VA Medical Center (Minneapolis, MN).

Euthanasia, processing of tissue and micro-computed tomography (μCT)

Mice were sacrificed with CO_2 delivered via compressed gas cylinder and perfused intracardially with 20 ml of 0.1 M phosphate buffered saline (PBS, pH = 7.4 at 4°C) followed by 20 ml of 4% formaldehyde/12.5% picric acid solution in 0.1M PBS. Mouse femurs were removed following perfusion of mice as previously described (Peters et al., 2005). Tissues were post-fixed for 4 hours in the perfusion fixative solution and subsequently placed in 0.1M PBS prior to analysis.

In order to obtain a three dimensional image of the femur, bones were analysed with an eXplore Locus SP micro-computed tomographer (GE Healthcare). This conebeam μCT scanner uses a 2300 × 2300 CCD detector with current and voltage set at 80 μA and 80 kVp, respectively. Specimens were scanned in 1080 views through 360° with a 2100 ms integration time. Scans were then reconstructed at 16-μm^3 resolution using Reconstruction Utility software (GE Healthcare; London, Ontario, Canada) and visualized with Microview software (GE Healthcare; London, Ontario, Canada).

After μCT analysis, femora were rinsed with PBS and decalcified in 10% EDTA at 4ºC. EDTA was changed once a week for two weeks or until total decalcification, which was radiographically monitored using a Faxitron MX20 cabinet X-ray (Faxitron X-Ray Corporation, Wheeling, IL, USA) and Kodak Min-R 2000 film (Eastman Kodak Co., Windsor, CO, USA). After the desired demineralization, bones were cryoprotected in 30% sucrose at 4°C for at least 48 hours.

Immunohistochemistry on sectioned tissue

For immunohistochemistry, sections (20 μm thick) were cut on a cryostat and thaw-mounted on gelatin-coated slides for processing. Sections of the femur were dried at room temperature (RT) for 30 min, washed in 0.1M PBS three times for 10 min each (3×10), blocked with 3% normal donkey serum (NDS; Jackson ImmunoResearch, West Grove, PA, USA) in PBS with 0.3% Triton-X 100 for 60 min and then incubated overnight with primary antibodies made in 1% NDS and 0.1% Triton-X 100 in 0.1M PBS at RT. A variety of antibodies (Table 1) were used to identify different populations of nerve fibers that express TrkA. In order to identify all nerve profiles we used an antibody raised against protein gene product 9.5 (PGP 9.5). Peptide-rich and myelinated primary afferent sensory nerve fibers were labeled with antibodies raised against calcitonin gene-related peptide (CGRP) and neurofilament 200 kDa (NF200), respectively. Nerve fibers were labeled with an antibody raised against growth associated protein 43 (GAP43) and sympathetic nerve fibers were stained with an antibody raised against tyrosine hydroxylase (TH). The primary antibody cocktails used for double-label immunohistochemistry included: PGP 9.5/TrkA, CGRP/TrkA, NF200/TrkA, CGRP/GAP43 and NF200/GAP43. Detailed description of the primary antibodies is provided in the Table 1. The following day, preparations were washed 3×10 min each in PBS and incubated for three hours at RT with secondary antibodies conjugated to fluorescent markers (Cy3/Cy2; 1:600/1:200; Jackson ImmunoResearch, West Grove, PA, USA). Preparations were then washed 3×10 min each in PBS and counterstained with DAPI

(4′, 6-diamidino-2-phenyl-indole, dihydrochloride, 1:30000, Molecular Probes, OR, USA) for 5 min. Finally, sections were washed 3X10 min each in PBS and dehydrated through an alcohol gradient (70, 80, 90 and 100%), cleared in xylene, and coverslipped with di-n-butylphthalate-polystyrene-xylene (Sigma Chemical Co., St. Louis, MO, USA). Preparations were allowed to dry at RT for 12 hours before imaging.

Immunohistochemistry on whole-mount preparations of the femoral periosteum

As previously described the periosteum from the diaphyseal shaft was removed as a whole mount preparation (Brownlow et al 2000) and processed for immunohistochemistry as previously reported (Ghilardi et al., 2010a, Jimenez-Andrade et al., 2010b, Mantyh et al., 2010). Briefly, excess muscle was removed from the femur using surgical scissors (Cat # 14004110, Fine Science Tools Inc, Foster City, CA, USA) without disturbing the bone and attached periosteum. The periosteum was harvested from the distal growth plate region to immediately below the third trochanter. The periosteum was removed from the bone by tracing the lower and upper limits of the desired area with a stainless steel surgical blade No. 11 (Feather Safety Razor, Co, Kita-Ku, Osaka, Japan) and a vertical cut was then performed along the posterior surface of the bone. Under a dissecting microscope, the periosteum was removed by gently scraping against the bone using the edge of a forceps (Dumont # 5/45, Fine Science Tools Inc, Foster City, CA, USA) (Brownlow et al., 2000). During the periosteal removal, femurs were continually irrigated with PBS to prevent tissue dehydration. The whole-mount preparations of the periosteum were then washed in 0.1M PBS 3×10 min each, incubated for 60 min at RT in a blocking solution of 3% NDS in PBS with 0.3% Triton-X 100 and then the preparations were incubated with a cocktail of PGP 9.5/TrkA primary antibodies overnight at RT. After incubation with primary antibodies, the same immunohistochemical procedure was followed as is previously described for frozen sections.

While we and previous authors (see Table 1 for references) believe the antibodies used in the present study represent staining of the specific antigen being targeted, we use the ($^+$) convention (i.e. TrkA$^+$), which we define as like-immunoreactivity.

Laser Confocal Microscopy

Images were acquired with an Olympus Fluoview FV1000 microscope that is equipped with different lasers (Multiline argon (458, 488, 515 nm), Green HeNe (543 nm), Red HeNe (633 nm), and Blue Diode (405 nm)) and multiple excitation and emission fluorescence filters. Confocal *z*-series were acquired at 0.5 μm intervals for each observation area. Sequential acquisition mode was used to reduce bleed-through from fluorophores. Image threshold and channel pseudocolors were adjusted with Adobe Photoshop CS and thereafter assembled in Adobe Illustrator CS4. For quantitative analysis, three images per bone compartment (periosteum, mineralized bone, and bone marrow) per animal were acquired (600× magnification) with a minimum of five animals per staining group. The density of DAPI$^+$ cells was used as a reference to acquire confocal images of the different bone compartments. For illustration purposes representative confocal images of the TrkA$^+$ nerve fibers from periosteal whole mount preparations were acquired and overlaid onto a three-dimensional μCT image of the mouse femur using Amira software (Visage Imaging, Inc. San Diego, CA, USA).

Quantification of the density of sensory nerve fibers innervating the different compartments of bone and the percentage of these nerve fibers that co-express TrkA

For quantification, cross sectional images of the whole bone sections were used, as the cross sections allow visualization of the bone's landmarks (such as the growth plate), which enable the observer to locate the same anatomical area when quantifying different animals.

For each given marker, 3 images were obtained per animal. The area evaluated was within a 1 mm-long segment initiated 2 mm proximal to the distal growth plate, with images taken from different sections at least 0.1 mm apart. The volume of the periosteum, bone marrow or mineralized bone that was analyzed was an average 400 μm (length), 70 μm (width), 20 μm (depth). The Z-stacked images were analyzed with Image-Pro Plus v. 6.0 (Media Cybernetics) and nerve fibers were manually traced to determine the length of nerve fibers. Density of nerve fibers was expressed as length of nerve fibers per volume of tissue (mm/mm^3) (Mantyh et al., 2010).

Quantitative analysis of the % of CGRP and NF200 nerve fibers co-expressing TrkA was adapted from previous methodologies (Herrero-Herranz et al., 2008, Kozsurek et al., 2009). Images were acquired with a 60× objective, under which it was possible to distinguish individual axons. The confocal z-stack images from double-stained bone sections were saved separately as TIFF files and visualized using Adobe Photoshop. The number of nerve fibers expressing a specific marker was determined in their respective confocal image. Then, images were overlaid to determine the number of nerve fibers that co-localize both markers. In order to exclude possible false double-labeling, single confocal plane images of the different phenotype markers were visualized through their entire z-axis in 0.5 μm steps.

Statistical analysis

All data are presented as mean ± standard error of the mean (SEM) Data were subsequently analyzed using a one-way analysis of variance (ANOVA), and Students Newman Keuls test was used for planned comparisons. The level of significance was set at $p < 0.05$.

RESULTS

Density and morphology of sensory nerve fibers innervating different bone compartments

The density of sensory nerve fibers innervating naïve periosteum was determined using two techniques: whole-mount preparations (which give a “bird’s eye-view” of the entire periosteum) and frozen sections (which provide a longitudinal cross sectional view of the periosteum). Confocal images of whole mount preparations of the femoral periosteum demonstrated that this tissue is densely innervated as is evidenced by the high number of PGP 9.5$^+$ nerve fibers that formed a complex mesh-like network (Fig 1A). In frozen sections, we observed CGRP$^+$ and NF200$^+$ sensory nerve fibers throughout the periosteum. These fibers have a linear and bifurcating pattern and can be found as single nerve fibers or nerve bundles. Additionally, the majority of CGRP$^+$ nerve fibers exhibited a beaded appearance and were thinner than NF200$^+$ nerve fibers (Fig 2B, 2D).

In the normal mineralized bone and bone marrow, both unmyelinated (Fig 4C and 5C) and myelinated (Fig 4E and 5E) sensory nerve fibers were also present. CGRP$^+$ and NF200$^+$ nerve fibers were evenly distributed and ran longitudinally into these bone compartments as contiguous fibers generally associated with the vasculature. These fibers were found as single or bundled fibers and had a linear morphology. CGRP$^+$ nerve fibers located in the bone marrow and mineralized bone also exhibited a beaded appearance (Hill and Elde, 1991). Additionally, we observed that normal articular cartilage of the distal femur and proximal tibia is not innervated by PGP 9.5$^+$, CGRP$^+$ or NF200$^+$ sensory nerve fibers (Data not shown).

Quantitative analysis showed that the various bone compartments have different densities of sensory nerve fibers. The density of CGRP$^+$ (2225 ± 318 mm/mm^3) and NF200$^+$ (1802 ± 145 mm/mm^3) nerve fibers was greatest in the periosteum, followed by bone marrow (CGRP: 61 ± 6 mm/mm^3; NF200: 41 ± 4.6 mm/mm^3). Finally, mineralized bone exhibited a low density of CGRP$^+$ (3.2 ± 0.7 mm/mm^3) and NF200$^+$ (3.7 ± 0.7 mm/mm^3) nerve fibers

(Table 2). These results demonstrate that the relationship of the density of $CGRP^+$ and $NF200^+$ sensory nerve fibers innervating the femur is periosteum > bone marrow > mineralized bone > cartilage, with a relative density of 100: 2.0: 0.1: 0.

TrkA is highly expressed in sensory and sympathetic nerve fibers that innervate the periosteum, bone marrow and mineralized bone

We also qualitatively and quantitatively determined the expression of TrkA in sensory nerve fibers that innervate the different bone compartments. Immunohistochemical analysis revealed that TrkA is expressed in the majority of the PGP 9.5^+ nerve fibers innervating the periosteum (Fig 1B, 1C). Overlaying confocal images of $TrkA^+$ nerve fibers on a reconstructed 3D image of the femur (μCT) allows for a better appreciation of the high density of $TrkA^+$ nerve fibers in the periosteum, which form a mesh-like network that entirely envelops all but the articulated surface of the mineralized bone (Fig 2A). These $TrkA^+$ nerve fibers exhibited different morphologies and patterns. While some nerve fibers have a linear or branching pattern of varying thickness, other fibers had a corkscrew-like morphology, which appeared to enwrap blood vessels. Staining of bone sections with markers of TrkA and TH showed that nearly all $TrkA^+$ nerve fibers with this corkscrew-like morphology were TH^+ (Fig 3). Double-labeled immunohistochemistry using frozen sections of the mouse femur confirmed that the TrkA receptor is expressed by $CGRP^+$ and $NF200^+$ nerve fibers in the periosteum (Fig 2), mineralized bone (Fig 4) and bone marrow (Fig 5). Quantitative analysis revealed that the percentage of $CGRP^+$ and $NF200^+$ nerve fibers expressing the TrkA receptor was over 80% and 50%, respectively, in the periosteum. In mineralized bone and bone marrow, over 80% of both $CGRP^+$ and $NF200^+$ fibers express TrkA (Table 2). These results suggested that the TrkA receptor is expressed by the majority of myelinated/unmyelinated sensory and sympathetic nerve fibers that innervate the periosteum, bone marrow and mineralized bone.

The majority of $CGRP^+$ and $NF200^+$ nerve fibers innervating bone express GAP43

Figure 6 shows that many $CGRP^+$ and $NF200^+$ nerve fibers that innervate the mouse periosteum co-express GAP43. Quantitative analysis revealed that 93.7 ± 1.6% of $CGRP^+$ nerve fibers express $GAP43^+$ and 93 ± 2.1% of $NF200^+$ nerve fibers express GAP43.

DISCUSSION

Populations of sensory nerve fibers that innervate the skin vs. skeleton

Previous studies have shown that the human and rodent skin is innervated by thickly myelinated nerve fibers (A-beta), thinly myelinated sensory nerve fibers (A-delta) and both classes of unmyelinated C-fibers: the peptide-rich $CGRP^+$ nerve fibers and peptide-poor nerve fibers (Karanth et al., 1991, Schulze et al., 1997, Zylka et al., 2005, Albrecht et al., 2006, Taylor et al., 2009). In contrast, the present report demonstrates that bone is innervated primarily by thinly myelinated sensory nerve fibers (A-delta) and peptide-rich $CGRP^+$ nerve fibers and thus has less “redundancy” than is found in skin (summarized in Fig 7). In the present study, it was also found that while the different bone compartments of the femur (periosteum, mineralized bone and bone marrow) were all innervated by both $CGRP^+$ and $NF200^+$ sensory nerve fibers, the density per unit volume of the sensory innervation of the different compartments were markedly different so that the approximate relative density of CGRP, NF200 or TrkA fibers was 100: 2: 0.1: 0 in the periosteum, marrow, mineralized bone and cartilage, respectively.

The data presented here are in agreement with previous electron microscopy studies that characterized the nerve fibers innervating the periosteum of the cat humerus (Ivanusic et al., 2006) and the bone marrow of the dog tibia (Seike, 1976). These studies demonstrated that

bone is primarily innervated by unmyelinated and thinly myelinated nerve fibers with few, if any, thickly myelinated nerve fibers. Similarly, electrophysiological recordings performed on nerve fibers entering the nutrient foramen of the humerus of the cat demonstrated that the conduction of nerve fibers separated into two categories, those with conduction velocities of less that 2m/s (presumably C-fibers) and those with conduction velocities between 2–30 m/s (presumably A-delta fibers) with no nerve fibers having conduction velocities >30m/s, which would correspond to A-beta fibers (Mahns et al., 2006).

Previous studies using either transgenic animals or retrograde tracers that were applied to different compartments of the skeleton also demonstrated the peptide poor population of C-fibers, that richly innervates the skin, does not appear to innervate the: human (Ozawa et al., 2006) and rat intervertebral discs (Ozawa et al., 2003, Aoki et al., 2005, Ohtori et al., 2007); rat hip (Nakajima et al., 2008); rat wrist joint (Kuniyoshi et al., 2007); rat knee and humerus (Kruger et al., 1989); or the mouse femur (Zylka et al., 2005, Jimenez-Andrade et al., 2010b). These results, together with the present study, suggest that the skeleton is innervated primarily by $NF200^+$ (presumably A-delta) and $CGRP^+$ (presumably A-delta or peptide-rich C-fibers) and that the majority of both of these populations of nerve fibers also express TrkA. These results also suggest that select populations of sensory nerve fibers innervate the skeleton and targeting this restricted population may provide a unique therapeutic opportunity for developing novel analgesics that can attenuate acute and chronic skeletal pain.

Sprouting and pathological reorganization of $TrkA^+$ nerve fibers in skeletal injury/disease

The present study indicates that most unmyelinated and myelinated sensory nerve fibers that innervate the skeleton also express GAP43 which is a protein thought to be involved in axonal growth and regeneration (Benowitz et al., 1987), nerve sprouting, and synaptic plasticity (Benowitz and Routtenberg, 1997). This result is in marked contrast to the human skin where studies reported that GAP43 was found in C-fibers, but not in $NF200^+$ nerve fibers. These findings lead the authors to suggest that in the skin, whereas C-fiber endings may be constantly remodeling, $NF200^+$ nerve fiber endings may be relatively stable (Albrecht et al., 2006).

In the bone there are at least two possible explanations as to why nearly all sensory nerve fibers express GAP43. First, in the young adult, bone is a tissue that is constantly remodeling, so that even under normal physiological conditions the nerve fibers must be continually remodeled within and around the newly resorbed and newly formed bone. Secondly, it has been previously shown that cell bodies of normal, uninjured adult sensory neurons that have high basal levels of mRNA coding for GAP43 also express high levels of TrkA (Verge et al., 1990). One speculation is that high basal concentration of GAP43 confers upon sensory neurons an increased capacity for collateral sprouting (Verge et al., 1990) perhaps in response to injury and/or disease. Indeed, reports have clearly demonstrated that nerve fibers innervating the skeleton have a remarkable capacity to undergo sprouting in both malignant and non-malignant disease.

In malignant skeletal disease (bone cancer) a recent study showed that when osteosarcoma cells grew within the bone, there was a remarkable sprouting and formation of neuroma-like structures by $TrkA^+$ sensory and sympathetic nerve fibers in the periosteum. Interestingly, sustained administration of an anti-NGF sequestering therapy largely blocked the pathological sprouting of sensory and sympathetic nerve fibers, the formation of neuroma-like structures, and significantly inhibited the generation and maintenance of cancer pain in this model (Mantyh et al., 2010). Similarly, recent studies using canine prostate cells injected into the mouse bone, which develop sclerotic lesions similar to that found in human prostate tumor bearing bones, demonstrated that $TrkA^+$ sensory and sympathetic nerve

fibers innervating the bone marrow also undergo a truly remarkable and pathological sprouting (Jimenez-Andrade et al., 2010a). Interestingly, these prostate cells do not express detectable levels of mRNA coding for NGF (Halvorson et al., 2005), suggesting that this ectopic sprouting of $TrkA^+$ nerve fibers is not driven by NGF released from tumor cells but NGF released by endogenous stromal, inflammatory and immune cells (Ehrhard et al., 1993, Skaper et al., 2001, Artico et al., 2008). These data demonstrate that even in the adult bone marrow, NGF released by these endogenous cells can induce a 10–70 fold increase in the density of $TrkA^+$ sensory nerve fibers in the bone marrow. As described below, these newly sprouted nerve fibers are probably also activated and sensitized by released NGF and as such this truly ectopic and pathological reorganization of $TrkA^+$ nerve fibers may provide an anatomical substrate which drives skeletal pain. In support of this hypothesis, preventive treatment with an antibody that sequesters NGF, administered when prostate tumor-induced pain and bone remodeling were first observed, blocked this ectopic sprouting and significantly attenuated the development and severity of cancer pain.

Sprouting of presumably $TrkA^+$ nerve fibers has also been observed in non-malignant skeletal pain states in both human and animals. For example, previous studies have reported that in human chronic discogenic pain may in part be due to a growth of $CGRP^+$ nerve fibers into normally aneural and avascular areas of the human intervertebral disc (Freemont et al., 2002). Other studies have demonstrated significant sprouting of $CGRP^+$ nerve fibers following bone fracture in rat and in the arthritic joints of humans and animals (Buma et al., 1992, Wu et al., 2002, Suri et al., 2007, Ashraf et al., 2010). These reports suggest that following injury or disease of the skeleton, significant sprouting of $TrkA^+$ nerve fibers can occur, and it appears that endogenous stromal cells as well as inflammatory and immune cells are the source of NGF (Ehrhard et al., 1993, Skaper et al., 2001, Artico et al., 2008). These data also suggest that $TrkA^+$ nerve fibers that normally innervate the skeleton may be pivotally involved in driving chronic hypersensitivity and allodynia following injury or disease in both non-malignant and malignant skeletal diseases.

Activation and sensitization of $TrkA^+$ sensory nerve fibers by NGF

While NGF induced sprouting of $TrkA^{+/}GAP43^+$ sensory fibers appears to be involved in driving skeletal pain, previous studies have clearly demonstrated that NGF binding to TrkA in peripheral tissues can play a pivotal role in the generation and maintenance of pain. In several animal and human models of pain, administration of NGF has been shown to induce acute pain and blockade of NGF or TrkA has been shown to attenuate this pain.

Cutaneous administration of NGF to rodents (Andreev et al., 1995) and to humans (Dyck et al., 1997) causes hyperalgesia within 1 or 3 hours, respectively, suggesting that NGF leads to sensitization of nociceptors. These relatively rapid effects are thought to be mediated primarily through NGF binding to TrkA expressed on mast cells, causing degranulation and release of a variety of algogenic mediators such as histamine, prostaglandin E2, serotonin (5-HT), hydrogen ions, and bradykinin, as well as additional NGF (Mendell et al., 1999), although the contributions of mast cells are not as clear in humans (Nilsson et al., 1997, Kulka et al., 2008). Also, NGF activation of $TrkA^+$ sensory nerve fibers leads to an increase in the expression of the neuropeptides including BDNF (Apfel et al., 1996, Priestley et al., 2002), CGRP and SP (Lindsay and Harmar, 1989, Lindsay et al., 1989). Additionally, in primary afferent sensory neurons NGF increases the phosphorylation and sensitization of transient receptor potential vanilloid 1 (TRPV1) (Winston et al., 2001, Zhang et al., 2005), sensitizes putative mechanotransducers (Di Castro et al., 2006), causes an upregulation of TrkA, p75 (Lindsay et al., 1990, Miller et al., 1991), TRPV1 (Ji et al., 2002), acid-sensing ion channels (ASICs), bradykinin receptor 2 (Lee et al., 2002), and TTX-resistant sodium channels (Gould et al., 2000, Kerr et al., 2001, Klein et al., 2003) and changes the currents of both calcium (Woodall et al., 2008) and potassium channels (Boettger et al., 2002).

Some of the most convincing evidence of the involvement of $TrkA^+$ nerve fibers in driving skeletal pain has come from *in vivo* animal and human experiments aimed at attenuating skeletal pain by blocking NGF or TrkA. Sequestration of NGF has been shown to reduce mouse (Inglis et al., 2008)**,** rat (Shelton et al., 2005) and human (Lane et al., 2010) arthritis pain, fracture pain in mice (Jimenez-Andrade et al., 2007), complex regional pain syndrome type I in rats (Sabsovich et al., 2008), and bone cancer pain due to sarcoma (Mantyh et al., 2010) or canine prostate tumor cells growing in mouse bones (Jimenez-Andrade et al., 2010a). Similarly, recent studies have reported the ability of TrkA inhibitors to attenuate mouse fracture pain (Ghilardi et al., 2010b) and mouse bone cancer pain (Ghilardi et al., 2010a) with similar efficacy (approximately a 50% reduction) as was seen with anti-NGF therapies in mouse and human studies thereby suggesting that it is the interaction of NGF with TrkA that drives skeletal pain.

Potential limitations and conclusions

This study had several potential limitations. First, this study examined the sensory innervation of mineralized bone, marrow, periosteum and cartilage of the mouse femur. In order to determine whether this pattern of innervation of the femur applies to all long and flat bones, additional studies will be needed. Second, decalcification of the bone using EDTA generally causes a decrease in the antigenicity of molecules in the bone tissue (Mullink et al., 1985, Schwei et al., 1999) resulting in an underestimation of nerve fibers that express a labile antigen such as TrkA or GAP43. However, studies performed in our lab show that the density of $TrkA^+$ nerve fibers in whole mount preparations that did not undergo decalcification is similar to those found in the periosteum of bone tissues that did undergo the standard decalcification treatment for 2 weeks. Third, the present study was conducted on femurs obtained from young, adult mice and these findings need to be confirmed in both middle-aged and old animals. Due to increased prevalence of skeletal diseases with aging, future studies are clearly needed to investigate how the density, phenotype and response characteristics of sensory nerve fibers that innervate bone change with age.

In conclusion, the majority of sensory nerve fibers in bone express TrkA which may in part explain why blockade of NGF or TrkA is effective in attenuating skeletal pain. Understanding how the density, morphology, phenotype and response characteristics of skeletal sensory nerve fibers change following injury, disease and aging, may help in the development of more targeted therapies to treat acute and/or chronic skeletal pain.

Acknowledgments

We thank Marvin Landis and the University of Arizona Information Technology Service for generating the 3D renderings of the innervated bone. This work was supported by the National Institutes of Health grant (NS23970), by the Department of Veteran Affairs, Veteran Health Administration, Rehabilitation Research and Development Service Grants (04380-I and A6707-R) and by the Calhoun Fund for Bone Pain. None of the authors of this study claim a conflict of interest. Gabriela Castañeda-Corral is a Conacyt fellow from Mexico.

LIST OF ABBREVIATIONS

μCT	Micro-computed tomography
5-HT	Serotonin
ANOVA	Analysis of variance
ASIC	Acid-sensing ion channels
BDNF	Brain-derived neurotrophic factor

CGRP	Calcitonin gene-related peptide
DAPI	4′, 6-diamidino-2-phenyl-indole
EDTA	Ethylenediaminetetraacetic acid
GAP43	Growth associated protein-43
GFP	Green fluorescent protein
NDS	Normal donkey serum
NF200	Neurofilament 200 kDa
NGF	Nerve growth factor
p75	p75 neurotrophin receptor
PBS	Phosphate buffered saline
PGP 9.5	Protein gene product 9.5
RT	Room temperature
SEM	Standard error of the mean
SP	Substance P
TH	Tyrosine hydroxylase
TrkA	Tropomyosin receptor kinase A
TRPV1	Transient receptor potential vanilloid 1
TTX	Tetrodotoxin

References

Aguilar C, Vichinsky E, Neumayr L. Bone and joint disease in sickle cell disease. Hematol Oncol Clin North Am. 2005; 19:929–941. viii. [PubMed: 16214653]

Albrecht PJ, Hines S, Eisenberg E, Pud D, Finlay DR, Connolly MK, Pare M, Davar G, Rice FL. Pathologic alterations of cutaneous innervation and vasculature in affected limbs from patients with complex regional pain syndrome. Pain. 2006; 120:244–266. [PubMed: 16427199]

Ambalavanar R, Moritani M, Dessem D. Trigeminal P2X3 receptor expression differs from dorsal root ganglion and is modulated by deep tissue inflammation. Pain. 2005; 117:280–291. [PubMed: 16153775]

Andreev N, Dimitrieva N, Koltzenburg M, McMahon SB. Peripheral administration of nerve growth factor in the adult rat produces a thermal hyperalgesia that requires the presence of sympathetic post-ganglionic neurones. Pain. 1995; 63:109–115. [PubMed: 8577480]

Aoki Y, Ohtori S, Takahashi K, Ino H, Douya H, Ozawa T, Saito T, Moriya H. Expression and co-expression of VR1, CGRP, and IB4-binding glycoprotein in dorsal root ganglion neurons in rats: differences between the disc afferents and the cutaneous afferents. Spine. 2005; 30:1496–1500. [PubMed: 15990662]

Apfel SC, Wright DE, Wiideman AM, Dormia C, Snider WD, Kessler JA. Nerve growth factor regulates the expression of brain-derived neurotrophic factor mRNA in the peripheral nervous system. Mol Cell Neurosci. 1996; 7:134–142. [PubMed: 8731481]

Artico M, Bronzetti E, Felici LM, Alicino V, Ionta B, Bronzetti B, Magliulo G, Grande C, Zamai L, Pasquantonio G, De Vincentiis M. Neurotrophins and their receptors in human lingual tonsil: an immunohistochemical analysis. Oncol Rep. 2008; 20:1201–1206. [PubMed: 18949422]

Ashraf S, Wibberley H, Mapp PI, Hill R, Wilson D, Walsh DA. Increased vascular penetration and nerve growth in the meniscus: a potential source of pain in osteoarthritis. Ann Rheum Dis. 2010

Bennett DL, Dmietrieva N, Priestley JV, Clary D, McMahon SB. TrkA, CGRP and IB4 expression in retrogradely labelled cutaneous and visceral primary sensory neurones in the rat. Neurosci Lett. 1996; 206:33–36. [PubMed: 8848275]

Benowitz LI, Perrone-Bizzozero NI, Finklestein SP. Molecular properties of the growth-associated protein GAP-43 (B-50). J Neurochem. 1987; 48:1640–1647. [PubMed: 3559571]

Benowitz LI, Routtenberg A. GAP-43: an intrinsic determinant of neuronal development and plasticity. Trends in Neurosciences. 1997; 20:84–91. [PubMed: 9023877]

Bjurholm A, Kreicbergs A, Brodin E, Schultzberg M. Substance P- and CGRP-immunoreactive nerves in bone. Peptides. 1988; 9:165–171. [PubMed: 2452430]

Boettger MK, Till S, Chen MX, Anand U, Otto WR, Plumpton C, Trezise DJ, Tate SN, Bountra C, Coward K, Birch R, Anand P. Calcium-activated potassium channel SK1- and IK1-like immunoreactivity in injured human sensory neurones and its regulation by neurotrophic factors. Brain. 2002; 125:252–263. [PubMed: 11844726]

Brownlow HC, Reed A, Joyner C, Simpson AH. Anatomical effects of periosteal elevation. J Orthop Res. 2000; 18:500–502. [PubMed: 10937640]

Buma P, Verschuren C, Versleyen D, Van der Kraan P, Oestreicher AB. Calcitonin gene-related peptide, substance P and GAP-43/B-50 immunoreactivity in the normal and arthrotic knee joint of the mouse. Histochemistry. 1992; 98:327–339. [PubMed: 1283163]

Di Castro A, Drew LJ, Wood JN, Cesare P. Modulation of sensory neuron mechanotransduction by PKC- and nerve growth factor-dependent pathways. Proc Natl Acad Sci U S A. 2006; 103:4699–4704. [PubMed: 16537426]

Dominick KL, Ahern FM, Gold CH, Heller DA. Health-related quality of life and health service use among older adults with osteoarthritis. Arthritis Rheum. 2004; 51:326–331. [PubMed: 15188315]

Doran JF, Jackson P, Kynoch PA, Thompson RJ. Isolation of PGP 9.5, a new human neurone-specific protein detected by high-resolution two-dimensional electrophoresis. J Neurochem. 1983; 40:1542–1547. [PubMed: 6343558]

Dyck PJ, Peroutka S, Rask C, Burton E, Baker MK, Lehman KA, Gillen DA, Hokanson JL, O'Brien PC. Intradermal recombinant human nerve growth factor induces pressure allodynia and lowered heat-pain threshold in humans. Neurology. 1997; 48:501–505. [PubMed: 9040746]

Ehrhard PB, Erb P, Graumann U, Otten U. Expression of nerve growth factor and nerve growth factor receptor tyrosine kinase Trk in activated CD4-positive T-cell clones. Proc Natl Acad Sci U S A. 1993; 90:10984–10988. [PubMed: 7902578]

Freemont AJ. The cellular pathobiology of the degenerate intervertebral disc and discogenic back pain. Rheumatology (Oxford). 2009; 48:5–10. [PubMed: 18854342]

Freemont AJ, Watkins A, Le Maitre C, Baird P, Jeziorska M, Knight MT, Ross ER, O'Brien JP, Hoyland JA. Nerve growth factor expression and innervation of the painful intervertebral disc. J Pathol. 2002; 197:286–292. [PubMed: 12115873]

Ghilardi, JR.; Freeman, KT.; Jimenez-Andrade, JM.; Mantyh, GW.; Bloom, AP.; Kuskowski, MA.; Mantyh, PW. Administration of a tropomyosin receptor kinase inhibitor attenuates sarcoma-induced nerve sprouting, neuroma formation and bone cancer pain Molecular Pain. 2010a. p. 6

Ghilardi JR, Freeman KT, Jimenez-Andrade JM, Mantyh WG, Bloom AP, Bouhana KS, Trollinger D, Winkler J, Lee P, Andrews SW, Kuskowski MA, Mantyh PW. Sustained blockade of neurotrophin receptors TrkA, TrkB and TrkC reduces non-malignant skeletal pain but not the maintenance of sensory and sympathetic nerve fibers. Bone. 2010b

Giaccone G, Huizing M, ten Bokkel Huinink W, Koolen M, Postmus P, van Kralingen K, van Zandwijk N, Vermorken J, Beijnen J, Dalesio O, et al. Preliminary results of two dose-finding studies of paclitaxel (Taxol) and carboplatin in non-small cell lung and ovarian cancers: a European Cancer Centre effort. Semin Oncol. 1994; 21:34–38. [PubMed: 7939761]

Gibson SJ, Polak JM, Bloom SR, Sabate IM, Mulderry PM, Ghatei MA, McGregor GP, Morrison JF, Kelly JS, Evans RM, et al. Calcitonin gene-related peptide immunoreactivity in the spinal cord of man and of eight other species. J Neurosci. 1984; 4:3101–3111. [PubMed: 6209366]

Gould HJ 3rd, Gould TN, England JD, Paul D, Liu ZP, Levinson SR. A possible role for nerve growth factor in the augmentation of sodium channels in models of chronic pain. Brain Res. 2000; 854:19–29. [PubMed: 10784102]

Halvorson KG, Kubota K, Sevcik MA, Lindsay TH, Sotillo JE, Ghilardi JR, Rosol TJ, Boustany L, Shelton DL, Mantyh PW. A blocking antibody to nerve growth factor attenuates skeletal pain induced by prostate tumor cells growing in bone. Cancer Res. 2005; 65:9426–9435. [PubMed: 16230406]

Herrero-Herranz E, Pardo LA, Gold R, Linker RA. Pattern of axonal injury in murine myelin oligodendrocyte glycoprotein induced experimental autoimmune encephalomyelitis: implications for multiple sclerosis. Neurobiol Dis. 2008; 30:162–173. [PubMed: 18342527]

Hill EL, Elde R. Distribution of CGRP-, VIP-, DbH-, SP-, and NPY-immunoreactive nerves in the periosteum of the rat. Cell Tissue Res. 1991; 264:469–480. [PubMed: 1714353]

Hukkanen M, Konttinen YT, Rees RG, Santavirta S, Terenghi G, Polak JM. Distribution of nerve endings and sensory neuropeptides in rat synovium, meniscus and bone. Int J Tissue React. 1992; 14:1–10. [PubMed: 1383167]

Inglis JJ, McNamee KE, Chia SL, Essex D, Feldmann M, Williams RO, Hunt SP, Vincent T. Regulation of pain sensitivity in experimental osteoarthritis by the endogenous peripheral opioid system. Arthritis Rheum. 2008; 58:3110–3119. [PubMed: 18821665]

Ivanusic JJ, Mahns DA, Sahai V, Rowe MJ. Absence of large-diameter sensory fibres in a nerve to the cat humerus. J Anat. 2006; 208:251–255. [PubMed: 16441569]

Jeon SM, Lee KM, Park ES, Jeon YH, Cho HJ. Monocyte chemoattractant protein-1 immunoreactivity in sensory ganglia and hindpaw after adjuvant injection. Neuroreport. 2008; 19:183–186. [PubMed: 18185105]

Ji RR, Samad TA, Jin SX, Schmoll R, Woolf CJ. p38 MAPK activation by NGF in primary sensory neurons after inflammation increases TRPV1 levels and maintains heat hyperalgesia. Neuron. 2002; 36:57–68. [PubMed: 12367506]

Jimenez-Andrade JM, Bloom AP, Stake JI, Mantyh WG, Taylor RN, Freeman KT, Ghilardi JR, Kuskowski MA, Mantyh PW. Pathological sprouting of adult nociceptors in chronic prostate cancer-induced bone pain. J Neurosci. 2010a; 30:14649–14656. [PubMed: 21048122]

Jimenez-Andrade JM, Mantyh WG, Bloom AP, Xu H, Ferng AS, Dussor G, Vanderah TW, Mantyh PW. A phenotypically restricted set of primary afferent nerve fibers innervate the bone versus skin: Therapeutic opportunity for treating skeletal pain. Bone. 2010b; 46:306–313. [PubMed: 19766746]

Jimenez-Andrade JM, Martin CD, Koewler NJ, Freeman KT, Sullivan LJ, Halvorson KG, Barthold CM, Peters CM, Buus RJ, Ghilardi JR, Lewis JL, Kuskowski MA, Mantyh PW. Nerve growth factor sequestering therapy attenuates non-malignant skeletal pain following fracture. Pain. 2007; 133:183–196. [PubMed: 17693023]

Karanth SS, Springall DR, Kuhn DM, Levene MM, Polak JM. An immunocytochemical study of cutaneous innervation and the distribution of neuropeptides and protein gene product 9.5 in man and commonly employed laboratory animals. Am J Anat. 1991; 191:369–383. [PubMed: 1719791]

Kerr BJ, Souslova V, McMahon SB, Wood JN. A role for the TTX-resistant sodium channel Nav 1.8 in NGF-induced hyperalgesia, but not neuropathic pain. Neuroreport. 2001; 12:3077–3080. [PubMed: 11568640]

Kidd BL. Osteoarthritis and joint pain. Pain. 2006; 123:6–9. [PubMed: 16714085]

Kimura K, Kanazawa H, Ieda M, Kawaguchi-Manabe H, Miyake Y, Yagi T, Arai T, Sano M, Fukuda K. Norepinephrine-induced nerve growth factor depletion causes cardiac sympathetic denervation in severe heart failure. Auton Neurosci. 2010; 156:27–35. [PubMed: 20335077]

Klein JP, Tendi EA, Dib-Hajj SD, Fields RD, Waxman SG. Patterned electrical activity modulates sodium channel expression in sensory neurons. J Neurosci Res. 2003; 74:192–198. [PubMed: 14515348]

Kozsurek M, Lukacsi E, Fekete C, Puskar Z. Nonselective innervation of lamina I projection neurons by cocaine- and amphetamine-regulated transcript peptide (CART)-immunoreactive fibres in the rat spinal dorsal horn. Eur J Neurosci. 2009; 29:2375–2387. [PubMed: 19490082]

Kruger L, Silverman JD, Mantyh PW, Sternini C, Brecha NC. Peripheral patterns of calcitonin-gene-related peptide general somatic sensory innervation: cutaneous and deep terminations. JCompNeurol. 1989; 280:291–302.

Kulka M, Sheen CH, Tancowny BP, Grammer LC, Schleimer RP. Neuropeptides activate human mast cell degranulation and chemokine production. Immunology. 2008; 123:398–410. [PubMed: 17922833]

Kuniyoshi K, Ohtori S, Ochiai N, Murata R, Matsudo T, Yamada T, Ochiai SS, Moriya H, Takahashi K. Characteristics of sensory DRG neurons innervating the wrist joint in rats. Eur J Pain. 2007; 11:323–328. [PubMed: 16807014]

Lane NE, Schnitzer TJ, Birbara CA, Mokhtarani M, Shelton DL, Smith MD, Brown MT. Tanezumab for the treatment of pain from osteoarthritis of the knee. N Engl J Med. 2010; 363:1521–1531. [PubMed: 20942668]

Lawson SN, Waddell PJ. Soma neurofilament immunoreactivity is related to cell size and fibre conduction velocity in rat primary sensory neurons. J Physiol. 1991; 435:41–63. [PubMed: 1770443]

Lee YJ, Zachrisson O, Tonge DA, McNaughton PA. Upregulation of bradykinin B2 receptor expression by neurotrophic factors and nerve injury in mouse sensory neurons. Mol Cell Neurosci. 2002; 19:186–200. [PubMed: 11860272]

Lentz SI, Edwards JL, Backus C, McLean LL, Haines KM, Feldman EL. Mitochondrial DNA (mtDNA) Biogenesis: Visualization and Duel Incorporation of BrdU and EdU Into Newly Synthesized mtDNA In Vitro. J Histochem Cytochem. 2009

Lindsay RM, Harmar AJ. Nerve growth factor regulates expression of neuropeptide genes in adult sensory neurons. Nature. 1989; 337:362–364. [PubMed: 2911387]

Lindsay RM, Lockett C, Sternberg J, Winter J. Neuropeptide expression in cultures of adult sensory neurons: Modulation of substance P and calcitonin gene-related peptide levels by nerve growth factor. Neuroscience. 1989; 33:53–65. [PubMed: 2481245]

Lindsay RM, Shooter EM, Radeke MJ, Misko TP, Dechant G, Thoenen H, Lindholm D. Nerve Growth Factor Regulates Expression of the Nerve Growth Factor Receptor Gene in Adult Sensory Neurons. Eur J Neurosci. 1990; 2:389–396. [PubMed: 12106026]

Liu MT, Kuan YH, Wang J, Hen R, Gershon MD. 5-HT4 receptor-mediated neuroprotection and neurogenesis in the enteric nervous system of adult mice. J Neurosci. 2009; 29:9683–9699. [PubMed: 19657021]

Lu J, Zhou XF, Rush RA. Small primary sensory neurons innervating epidermis and viscera display differential phenotype in the adult rat. Neurosci Res. 2001; 41:355–363. [PubMed: 11755222]

Lubeck DP. The costs of musculoskeletal disease: health needs assessment and health economics. Best Pract Res Clin Rheumatol. 2003; 17:529–539. [PubMed: 12787516]

Mach DB, Rogers SD, Sabino MC, Luger NM, Schwei MJ, Pomonis JD, Keyser CP, Clohisy DR, Adams DJ, O'Leary P, Mantyh PW. Origins of skeletal pain: sensory and sympathetic innervation of the mouse femur. Neuroscience. 2002; 113:155–166. [PubMed: 12123694]

Mahns DA, Ivanusic JJ, Sahai V, Rowe MJ. An intact peripheral nerve preparation for monitoring the activity of single, periosteal afferent nerve fibres. J Neurosci Methods. 2006; 156:140–144. [PubMed: 16574241]

Mantyh WG, Jimenez-Andrade JM, Stake JI, Bloom AP, Kaczmarska MJ, Taylor RN, Freeman KT, Ghilardi JR, Kuskowski MA, Mantyh PW. Blockade of nerve sprouting and neuroma formation markedly attenuates the development of late stage cancer pain. Neuroscience. 2010; 171:588–598. [PubMed: 20851743]

McCarthy PW, Lawson SN. Cell type and conduction velocity of rat primary sensory neurons with calcitonin gene-related peptide-like immunoreactivity. Neuroscience. 1990; 34:623–632. [PubMed: 2352644]

McNamee KE, Burleigh A, Gompels LL, Feldmann M, Allen SJ, Williams RO, Dawbarn D, Vincent TL, Inglis JJ. Treatment of murine osteoarthritis with TrkAd5 reveals a pivotal role for nerve growth factor in non-inflammatory joint pain. Pain. 2010; 149:386–392. [PubMed: 20350782]

Mendell LM, Albers KM, Davis BM. Neurotrophins, nociceptors, and pain. Microscopy Research & Technique. 1999; 45:252–261. [PubMed: 10383118]

Miller FD, Mathew TC, Toma JG. Regulation of nerve growth factor receptor gene expression by nerve growth factor in the developing peripheral nervous system. JCell Biol. 1991; 112:303–312. [PubMed: 1671048]

Morrison RS, Magaziner J, McLaughlin MA, Orosz G, Silberzweig SB, Koval KJ, Siu AL. The impact of post-operative pain on outcomes following hip fracture. Pain. 2003; 103:303–311. [PubMed: 12791436]

Mullink H, Henzen-Logmans SC, Tadema TM, Mol JJ, Meijer CJ. Influence of fixation and decalcification on the immunohistochemical staining of cell-specific markers in paraffin-embedded human bone biopsies. J Histochem Cytochem. 1985; 33:1103–1109. [PubMed: 2414361]

Nakajima T, Ohtori S, Yamamoto S, Takahashi K, Harada Y. Differences in innervation and innervated neurons between hip and inguinal skin. Clin Orthop Relat Res. 2008; 466:2527–2532. [PubMed: 18704614]

Nilsson G, Forsberg-Nilsson K, Xiang Z, Hallbook F, Nilsson K, Metcalfe DD. Human mast cells express functional TrkA and are a source of nerve growth factor. Eur J Immunol. 1997; 27:2295–2301. [PubMed: 9341772]

Ohtori S, Inoue G, Koshi T, Ito T, Yamashita M, Yamauchi K, Suzuki M, Doya H, Moriya H, Takahashi Y, Takahashi K. Characteristics of sensory dorsal root ganglia neurons innervating the lumbar vertebral body in rats. J Pain. 2007; 8:483–488. [PubMed: 17382597]

Ozawa T, Aoki Y, Ohtori S, Takahashi K, Chiba T, Ino H, Moriya H. The dorsal portion of the lumbar intervertebral disc is innervated primarily by small peptide-containing dorsal root ganglion neurons in rats. Neurosci Lett. 2003; 344:65–67. [PubMed: 12781923]

Ozawa T, Ohtori S, Inoue G, Aoki Y, Moriya H, Takahashi K. The degenerated lumbar intervertebral disc is innervated primarily by peptide-containing sensory nerve fibers in humans. Spine. 2006; 31:2418–2422. [PubMed: 17023849]

Peleshok JC, Ribeiro-da-Silva A. Delayed reinnervation by nonpeptidergic nociceptive afferents of the glabrous skin of the rat hindpaw in a neuropathic pain model. J Comp Neurol. 2011; 519:49–63. [PubMed: 21120927]

Pelling M, Anthwal N, McNay D, Gradwohl G, Leiter AB, Guillemot F, Ang SL. Differential requirements for neurogenin 3 in the development of POMC and NPY neurons in the hypothalamus. Dev Biol. 2011

Peters CM, Ghilardi JR, Keyser CP, Kubota K, Lindsay TH, Luger NM, Mach DB, Schwei MJ, Sevcik MA, Mantyh PW. Tumor-induced injury of primary afferent sensory nerve fibers in bone cancer pain. Exp Neurol. 2005; 193:85–100. [PubMed: 15817267]

Priestley JV, Michael GJ, Averill S, Liu M, Willmott N. Regulation of nociceptive neurons by nerve growth factor and glial cell line derived neurotrophic factor. Can J Physiol Pharmacol. 2002; 80:495–505. [PubMed: 12056559]

Rosemann T, Laux G, Kuehlein T. Osteoarthritis and functional disability: results of a cross sectional study among primary care patients in Germany. BMC Musculoskelet Disord. 2007; 8:79. [PubMed: 17686172]

Sabsovich I, Wei T, Guo TZ, Zhao R, Shi X, Li X, Yeomans DC, Klyukinov M, Kingery WS, Clark JD. Effect of anti-NGF antibodies in a rat tibia fracture model of complex regional pain syndrome type I. Pain. 2008; 138:47–60. [PubMed: 18083307]

Sawatzky R, Liu-Ambrose T, Miller WC, Marra CA. Physical activity as a mediator of the impact of chronic conditions on quality of life in older adults. Health Qual Life Outcomes. 2007; 5:68. [PubMed: 18093310]

Schulze E, Witt M, Fink T, Hofer A, Funk RH. Immunohistochemical detection of human skin nerve fibers. Acta Histochem. 1997; 99:301–309. [PubMed: 9381913]

Schwei MJ, Honore P, Rogers SD, Salak-Johnson JL, Finke MP, Ramnaraine ML, Clohisy DR, Mantyh PW. Neurochemical and cellular reorganization of the spinal cord in a murine model of bone cancer pain. J Neurosci. 1999; 19:10886–10897. [PubMed: 10594070]

Seike W. Electrophysiological and histological studies on the sensibility of the bone marrow nerve terminal. Yonago Acta Med. 1976; 20:192–211. [PubMed: 1032858]

Sevcik MA, Ghilardi JR, Peters CM, Lindsay TH, Halvorson KG, Jonas BM, Kubota K, Kuskowski MA, Boustany L, Shelton DL, Mantyh PW. Anti-NGF therapy profoundly reduces bone cancer pain and the accompanying increase in markers of peripheral and central sensitization. Pain. 2005; 115:128–141. [PubMed: 15836976]

Shaw G, Yang C, Ellis R, Anderson K, Parker Mickle J, Scheff S, Pike B, Anderson DK, Howland DR. Hyperphosphorylated neurofilament NF-H is a serum biomarker of axonal injury. Biochem Biophys Res Commun. 2005; 336:1268–1277. [PubMed: 16176808]

Shelton DL, Zeller J, Ho WH, Pons J, Rosenthal A. Nerve growth factor mediates hyperalgesia and cachexia in auto-immune arthritis. Pain. 2005; 116:8–16. [PubMed: 15927377]

Skaper SD, Pollock M, Facci L. Mast cells differentially express and release active high molecular weight neurotrophins. Brain Res Mol Brain Res. 2001; 97:177–185. [PubMed: 11750074]

Song H, Stevens CF, Gage FH. Astroglia induce neurogenesis from adult neural stem cells. Nature. 2002; 417:39–44. [PubMed: 11986659]

Sugiura A, Ohtori S, Yamashita M, Inoue G, Yamauchi K, Koshi T, Suzuki M, Norimoto M, Orita S, Eguchi Y, Takahashi Y, Watanabe TS, Ochiai N, Takaso M, Takahashi K. Existence of nerve growth factor receptors, tyrosine kinase a and p75 neurotrophin receptors in intervertebral discs and on dorsal root ganglion neurons innervating intervertebral discs in rats. Spine (Phila Pa 1976). 2008; 33:2047–2051. [PubMed: 18758359]

Suri S, Gill SE, Massena de Camin S, Wilson D, McWilliams DF, Walsh DA. Neurovascular invasion at the osteochondral junction and in osteophytes in osteoarthritis. Ann Rheum Dis. 2007; 66:1423–1428. [PubMed: 17446239]

Taylor AM, Peleshok JC, Ribeiro-da-Silva A. Distribution of P2X(3)-immunoreactive fibers in hairy and glabrous skin of the rat. J Comp Neurol. 2009; 514:555–566. [PubMed: 19363794]

Thompson RJ, Doran JF, Jackson P, Dhillon AP, Rode J. PGP 9.5--a new marker for vertebrate neurons and neuroendocrine cells. Brain Res. 1983; 278:224–228. [PubMed: 6640310]

Verge VM, Tetzlaff W, Richardson PM, Bisby MA. Correlation between GAP43 and nerve growth factor receptors in rat sensory neurons. J Neurosci. 1990; 10:926–934. [PubMed: 2156965]

Wang ZZ, Stensaas LJ, Dinger B, Fidone SJ. Co-existence of tyrosine hydroxylase and dopamine beta-hydroxylase immunoreactivity in glomus cells of the cat carotid body. J Auton Nerv Syst. 1991; 32:259–264. [PubMed: 1709959]

Winston J, Toma H, Shenoy M, Pasricha PJ. Nerve growth factor regulates VR-1 mRNA levels in cultures of adult dorsal root ganglion neurons. Pain. 2001; 89:181–186. [PubMed: 11166474]

Wojtys EM, Beaman DN, Glover RA, Janda D. Innervation of the human knee joint by substance P fibers. Arthroscopy. 1990; 6:254–263. [PubMed: 1702291]

Woodall AJ, Richards MA, Turner DJ, Fitzgerald EM. Growth factors differentially regulate neuronal Cav channels via ERK-dependent signalling. Cell Calcium. 2008; 43:562–575. [PubMed: 17996937]

Woolf AD, Pfleger B. Burden of major musculoskeletal conditions. Bull World Health Organ. 2003; 81:646–656. [PubMed: 14710506]

Wu Z, Nagata K, Iijima T. Involvement of sensory nerves and immune cells in osteophyte formation in the ankle joint of adjuvant arthritic rats. Histochem Cell Biol. 2002; 118:213–220. [PubMed: 12271357]

Zahn PK, Subieta A, Park SS, Brennan TJ. Effect of blockade of nerve growth factor and tumor necrosis factor on pain behaviors after plantar incision. J Pain. 2004; 5:157–163. [PubMed: 15106128]

Zhang G, Dmitrieva N, Liu Y, McGinty KA, Berkley KJ. Endometriosis as a neurovascular condition: estrous variations in innervation, vascularization, and growth factor content of ectopic endometrial cysts in the rat. Am J Physiol Regul Integr Comp Physiol. 2008; 294:R162–171. [PubMed: 17942489]

Zhang X, Huang J, McNaughton PA. NGF rapidly increases membrane expression of TRPV1 heat-gated ion channels. EMBO J. 2005; 24:4211–4223. [PubMed: 16319926]

Zylka MJ, Rice FL, Anderson DJ. Topographically distinct epidermal nociceptive circuits revealed by axonal tracers targeted to Mrgprd. Neuron. 2005; 45:17–25. [PubMed: 15629699]

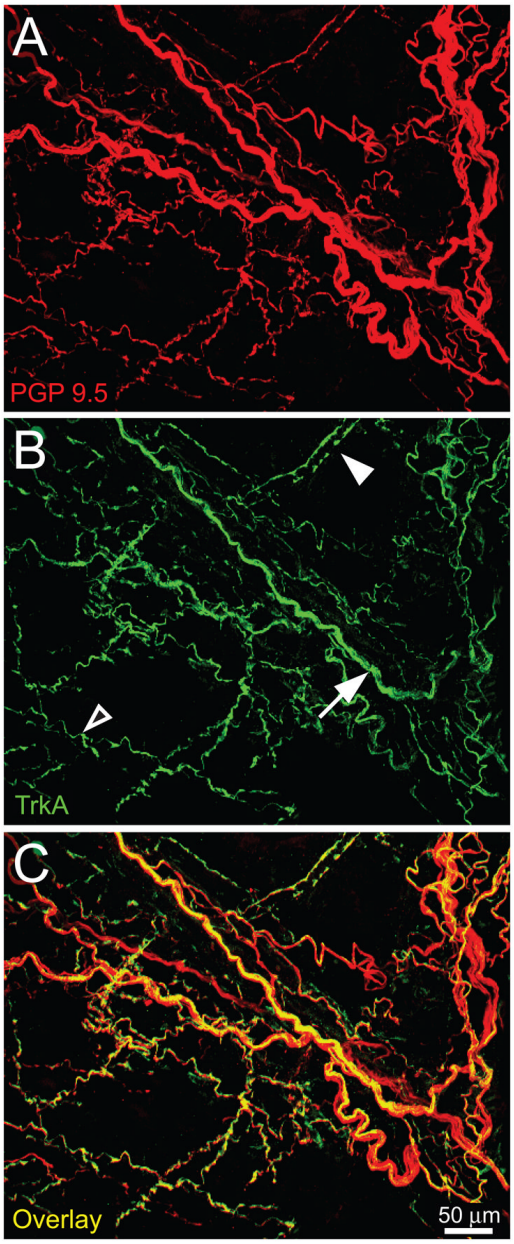

Figure 1.

The mouse femoral periosteum is densely innervated with tropomyosin receptor kinase A (TrkA) expressing nerve fibers. Confocal micrographs of whole mount preparations of the femoral periosteum of naïve mice that were immunohistochemically labeled with antibodies against protein gene product 9.5 (PGP 9.5, red in A) and with TrkA (green in B) and a merged image of (A) and (B) is presented in (C). PGP 9.5 is a pan-neuronal marker that is frequently used to label all nerve fibers that innervate a structure. In the periosteum or bone the majority of $PGP9.5^{+}$ nerve fibers express TrkA (C). Note that some $TrkA^{+}$ nerve fibers have a unique morphology corresponding to a specific type of nerve fiber: some are observed as single thin nerve fibers (empty arrowhead, probably a $CGRP^{+}$ C-fiber), bundles of thick nerve fibers (arrow, probably NF200 nerve fibers) and some appeared to enwrap blood vessels (filled arrowhead, probably TH^{+} sympathetic nerve fibers). Confocal images (30-µm z-series) were projected from 120 optical sections acquired at 0.25-µm intervals.

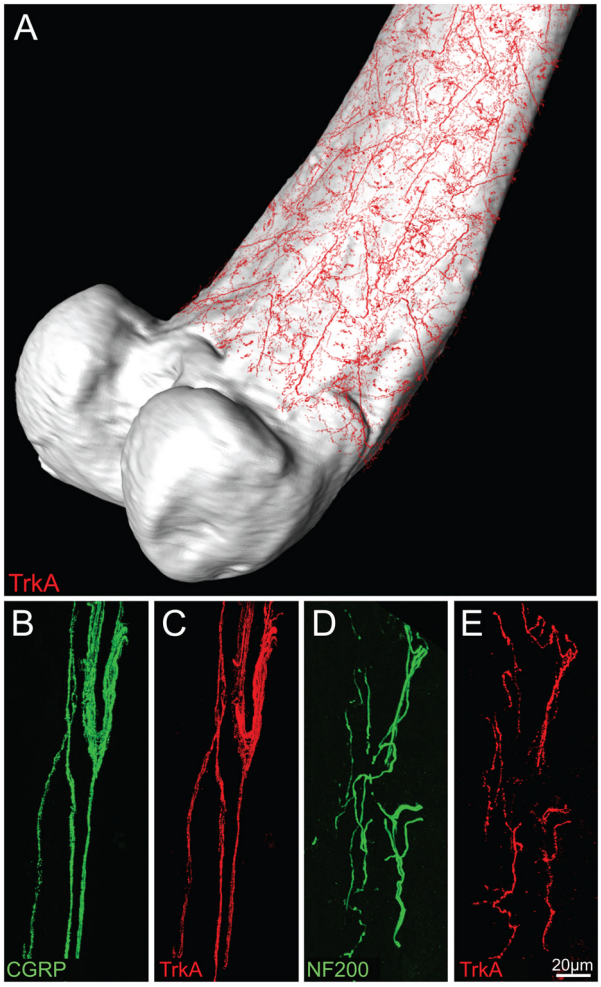

Figure 2.

There is a high density of TrkA$^+$ nerve fibers in the peristeum, which is a thin fibrous and cellular sheath that covers all but the articulated surface of the femur. For illustration purposes, representative confocal images of TrkA$^+$ nerve fibers (in red, A) which were obtained from periosteal whole mount preparations, were overlaid onto a three-dimensional μCT image of the femur using Amira software. Panels B–E are representative confocal images of the periosteum obtained from frozen bone sections (20-μm-thick) that were double-stained with antibodies against calcitonin gene-related peptide (CGRP, B)/TrkA (C); and neurofilament 200 kDa (NF200, D)/TrkA (E). CGRP is a neuropeptide found predominantly in unmyelinated (C-fibers) and some myelinated sensory nerve fibers, whereas NF200 is expressed predominantly by myelinated primary afferent sensory nerve fibers (McCarthy and Lawson, 1990; Lawson and Wandell, 1991). Note that the majority of CGRP$^+$ and NF200$^+$ nerve fibers that innervate the periosteum also express TrkA. Images in B–C and D–E are from the same bone section. Confocal images of periosteum were acquired at 0.5 μm *z*-plane intervals and the total z-plane was 20 μm.

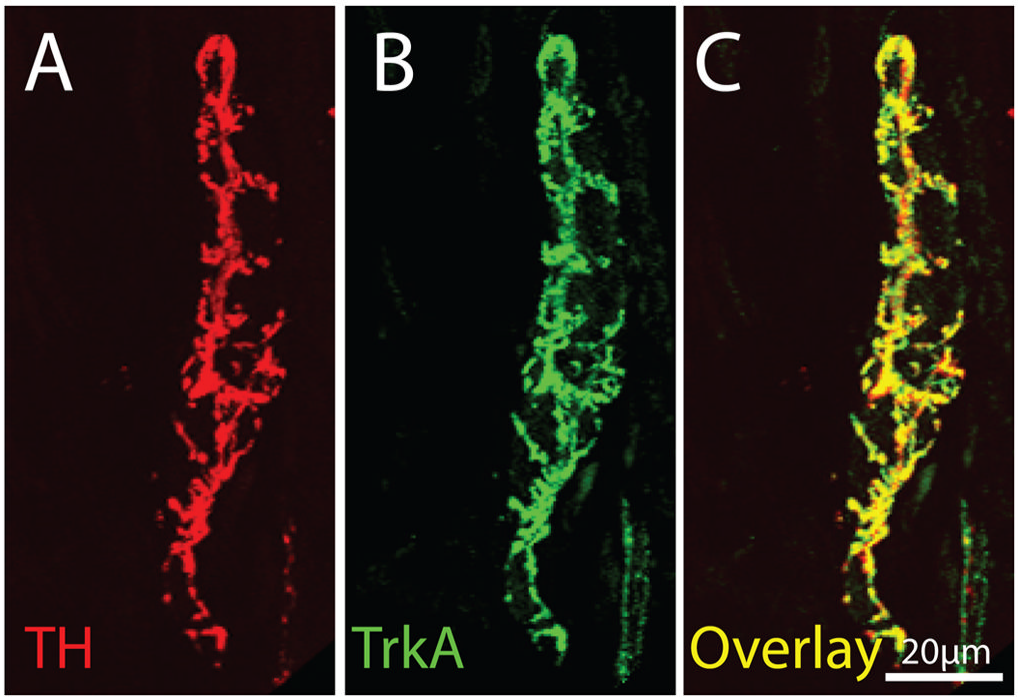

Figure 3.

The majority of TH^+ sympathetic nerve fibers that innervate the bone have a unique corkscrew appearance (as they wrap around blood vessels) and co-express TrkA. This figure contains confocal photomicrographs of periosteal frozen sections double-labeled with TH (A)/TrkA (B) and (C) is an overlay of (A) and (B). In mineralized bone and marrow one observes a similar co-localization in that nearly all TH^+ nerve fibers are $TrkA^+$. Images of periosteum were acquired from a frozen bone section (20-μm-thick) at 0.5 μm *z*-plane intervals and the total z-plane was 20 μm.

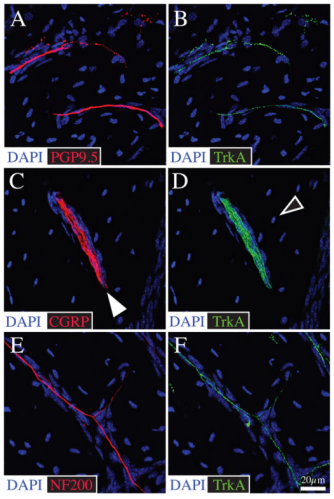

Figure 4.

$CGRP^+$ and $NF200^+$ sensory nerve fibers in bone primarily travel in the Haversian and Volkmann canals and great majority of these nerve fibers co-express TrkA. Representative confocal images of bone frozen sections (20-μm-thick) double stained with antibodies against PGP 9.5 (A)/TrkA (B), CGRP (C)/TrkA (D), and NF200 (E)/TrkA (F). In the mineralized bone, $CGRP^+$ and $NF200^+$ fibers are typically thin, have a linear appearance and sometimes form nerve bundles. These nerve fibers are generally associated with blood vessels located in the Haversian canals (filled arrowhead). The bone sections were counterstained with DAPI (a nuclear marker) that labels nuclei of resident osteocytes which are abundant in mineralized bone. Confocal images of mineralized bone were acquired at 0.5 μm *z*-plane intervals and the total z-plane was 20 μm.

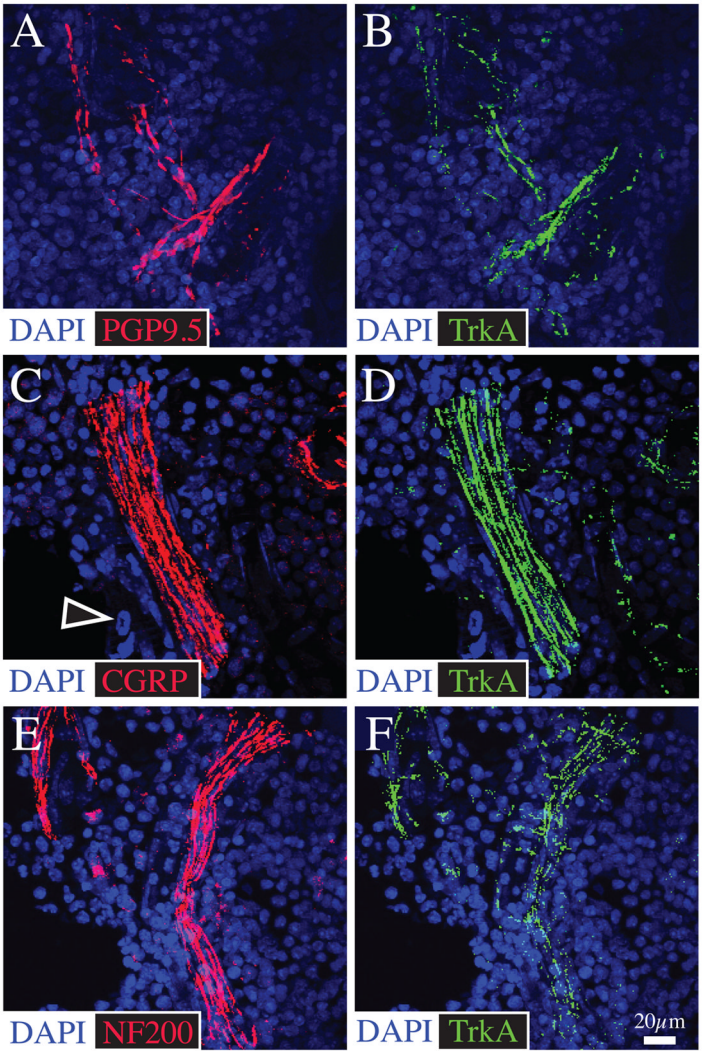

Figure 5.

Bone marrow is innervated by both CGRP$^+$ and NF200$^+$ sensory nerve fibers and the great majority of these nerve fibers in bone marrow express TrkA. Representative confocal images obtained from frozen sections of bone (20 μm-thick) double-stained with antibodies against PGP 9.5 (A)/TrkA (B); CGRP (C)/TrkA (D); and NF200 (E)/TrkA (F). The cells which contain DAPI stained nuclei (blue) are primarily hematopoietic and stromal cells which comprise the marrow. The empty arrowhead in C points to the DAPI stained nucleus of a hematopoietic cell. Confocal images of the bone marrow were acquired at 0.5 μm *z*-plane intervals and the total z-plane was 20 μm.

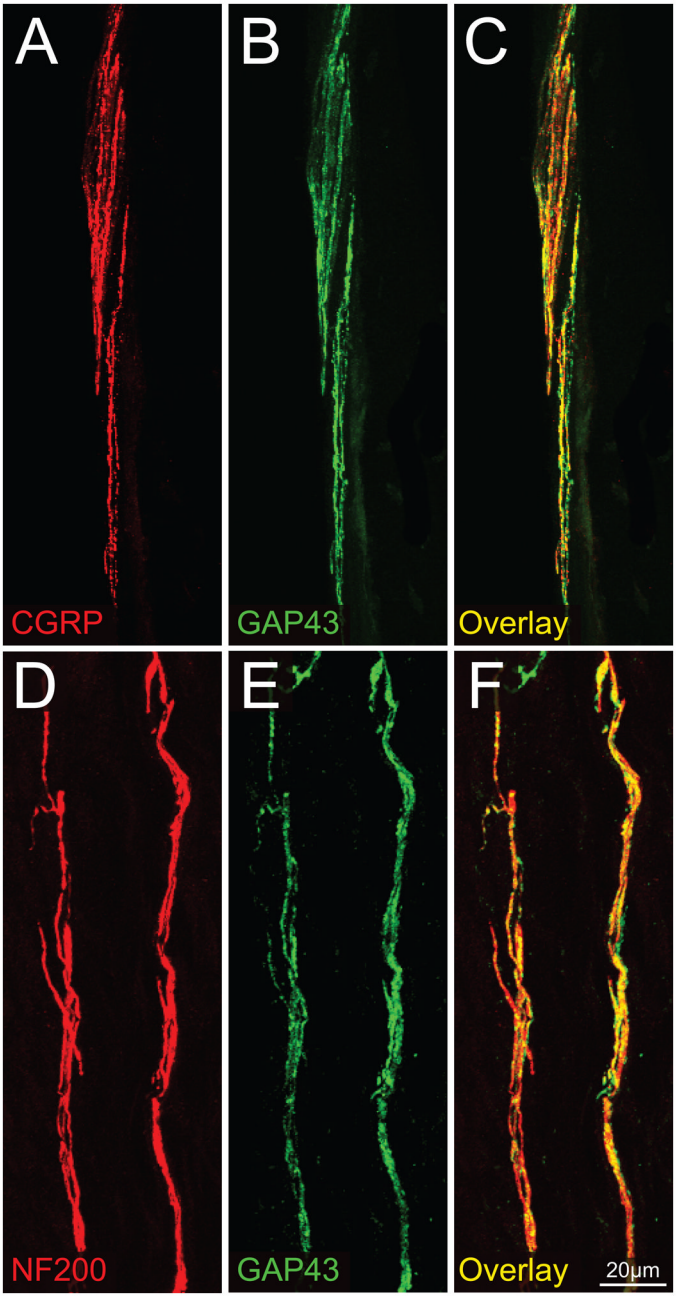

Figure 6.

Most NF200^{+} and CGRP^{+} sensory nerve fibers that innervate the bone also express growth associated protein 43 (GAP43). Confocal photomicrographs of periosteal frozen sections double labeled with CGRP (A)/GAP43 (B) and NF200 (D)/GAP43 (E). Panel (C) is an overlay of (A) and (B), while panel (F) is an overlay of (D) and (E). These data suggest that sensory nerve fibers that innervate the periosteum either are constantly remodeling and/or are capable of undergoing rapid sprouting and reorganization following bone injury or disease. Images of periosteum were acquired from a frozen bone sections (20-μm-thick) at 0.5 μm *z*-plane intervals and the total z-plane was 20 μm.

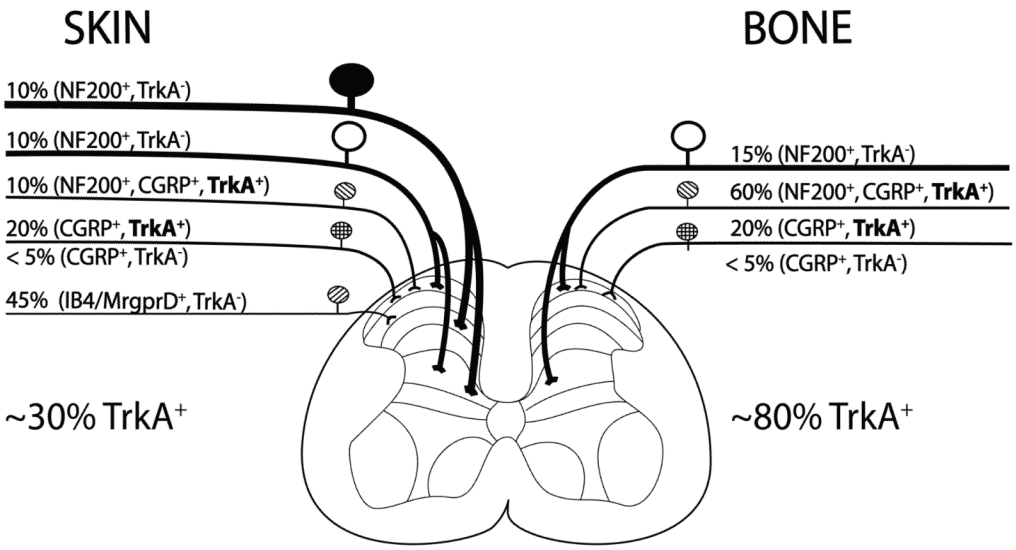

Figure 7.

Schematic illustrating the approximate percentage (%) and types of sensory nerve fibers that innervate the skin vs. bone. The skin is innervated by thickly myelinated A-beta fibers ($NF200^+$, $TrkA^-$), thinly myelinated A delta fibers ($NF200^+$, TkA^- and $NF200^+$, $CGRP^+$, $TrkA^+$), unmyelinated peptide-rich C fibers ($CGRP^+$, $TrkA^+$) and unmyelinated peptide-poor C-fibers (isolectin B_4 $(IB_4)^+$), *Mas related G protein-coupled receptor member D* $((Mrgprd)^+$, $TrkA^-$). In contrast, the bone appears to be predominantly innervated by thinly myelinated A-delta fibers ($NF\text{-}200^+$, $TrkA^-$ and $NF200^+$, $CGRP^+$, $TrkA^+$) and peptide-rich C-fibers ($CGRP^+$ and $TrkA^+$). In skin and bone there is also a small proportion (<5% of the total) of unmyelinated C-fibers that are $CGRP^+$, $TrkA^-$. The percentages and types of sensory nerve fibers innervating the skin were estimated using data from previous studies (Bennett et al., 1996, Lu et al., 2001, Ambalavanar et al., 2005, Zylka et al., 2005) and for bone from the present and previous studies (Nakajima et al., 2008, Sugiura et al., 2008, Jimenez-Andrade et al., 2010b). Note that whereas approximately 30% of the sensory nerve fibers that innervate skin are $TrkA^+$, greater than 80% of sensory nerve fibers that innervate the bone are $TrkA^+$.

Table 1

Background information on the antibodies used in this study.

Antigen	Immunogen	Manufacturer, Species raised in, Mono/ polyclonal, catalogue & lot number	Dilution used	Reference
CGRP	Synthetic rat Tyr-CGRP conjugated to keyhole limpet hemocyanin (37 amino acids)	Sigma Chemical Co., rabbit, polyclonal, Cat # C8198, Lot # 059K4841	1:10000	(Gibson et al., 1984) (Kruger et al., 1989) (Peleshok and Ribeiro-da-Silva, 2011)
NF200	NF-H isolated from bovine spinal cord (hyperphosphorylated, axonal form)	Neuromics, chicken, polyclonal, Cat # CH22104, Lot # 400719	1:5000	(Shaw et al., 2005) (Liu et al., 2009)
TrkA	NS0-derived recombinant rat TrkA extracellular domain (Amino acids 33–418)	R&D Systems, goat; polyclonal, Cat # AF1056, Lot # VFA0110031	1:50	(Zhang et al., 2008) (Jeon et al., 2008) (Lentz et al., 2009)
PGP 9.5	Human PGP9.5 protein emulsified in Freund's complete adjuvant (Complete sequence; 223 amino acids)	Ultraclone, rabbit, polyclonal, Cat # RA95101	1:4000	(Doran et al., 1983) (Thompson et al., 1983) (Peleshok and Ribeiro-da-Silva, 2011)
GAP 43	Recombinant rat GAP43 (complete sequence; 266 amino acids)	Millipore, rabbit, polyclonal, Cat # AB5220, Lot# NG1722291	1:1000	(Song et al., 2002) (Kimura et al., 2010)
TH	Tyrosine hydroxylase from rat pheochromocytoma denatured with sodium dodecyl sulfate (Complete sequence)	Millipore, rabbit, polyclonal, Cat # AB152, Lot# LV1591385	1:1000	(Wang et al., 1991) (Pelling et al. 2011)

Table 2

The density of $CGRP^+$ and $NF200^+$ sensory nerve fibers/unit volume in the different compartments of bone and the percent of these nerve fibers that co-express with TrkA. $CGRP^+$, $NF200^+$ and $TrkA^+$ were never detected in the normal, uninjured articular cartilage of the distal femur or proximal tibia.

Bone compartment	CGRP (mm/mm^3)	% of $CGRP^+$ nerve fibers that are $TrkA^+$	NF200 (mm/mm^3)	% of $NF200^+$ nerve fibers that are $TrkA^+$
Periosteum	2225 ± 318	90.6	1802 ± 145	54.8
Bone marrow	61 ± 6	87.8	41 ± 4.6	82.3
Mineralized bone	3.2 ± 0.7	97.1	3.7 ± 0.7	88.2